# A unified design proposal for shear stress prediction in crossing areas for cross laminated timber at in-plane shear and beam loading conditions

**Danielsson, Henrik; Jeleč, Mario**

Construction and Building Materials 355 (2022) 129167

Contents lists available at ScienceDirect

Construction and Building Materials

journal homepage: www.elsevier.com/locate/conbuildmat

# A unified design proposal for shear stress prediction in crossing areas for cross laminated timber at in-plane shear and beam loading conditions

Henrik Danielsson [a,*], Mario Jeleč [b]

[a] Division of Structural Mechanics, Lund University, P.O. Box 118, Lund SE-221 00, Sweden
[b] Faculty of Civil Engineering and Architecture Osijek, J. J. Strossmayer University of Osijek, Vladimira Preloga 3, 31000 Osijek, Croatia

ARTICLE INFO

*Keywords:*
CLT
Shear
In-plane
Wall
Beam
Unified design proposal
Crossing area

ABSTRACT

Environmental and urbanization challenges during the last few decades encouraged steady growth of mass timber construction where attention is drawn to cross laminated timber (CLT) as one of the most interesting products in terms of mechanical properties, versatility, efficient prefabrication and sustainability. Standardisation and codification regarding testing and design of CLT elements are hence pointed out as one of the main issues within the ongoing revision procedure of Eurocode 5. A consistent and unified design approach for CLT at pure in-plane shear loading conditions (shear walls) and at in-plane beam loading conditions is however still missing. This paper deals with analytical models for the determination of stress components related to predictions of load bearing capacity of CLT with respect to shear failure mode III – shear failure in the crossing areas constituted by the flatwise bonded areas between laminations of adjacent layers. This failure mode is relevant for both pure in-plane shear loading and in-plane beam loading conditions. The paper presents a review of previously proposed models for the prediction of shear stresses in crossing areas of CLT, for both loading conditions. Comparisons between FE-results and model predictions are reviewed indicating significant differences between them concerning the predicted influence of the CLT element lay-up and values of maximum shear stresses. Based on simplifications of models previously presented, a unified design proposal that is based on a rational and consistent mechanical background for both loading situations and that shows overall good agreement with FE-results is presented.

## 1. Background and introduction

In the pursuit to meet the increasing needs for housing, schools and offices and to decrease the environmental impact of the construction industry, attention is naturally drawn to wood-based structural materials. Today, cross laminated timber (CLT) is clearly one of the most interesting products in terms of mechanical properties, versatility, efficient prefabrication and environmental sustainability. During the recent 10 to 20 years, significant research efforts have been invested to gain an increased understanding of the structural behaviour of CLT and to develop reliable test methods and rationally based models for structural design [1,2]. Standardisation and codification regarding testing and design of CLT elements are pointed out as one of the main issues within the ongoing revision procedure of Eurocode 5.

The orthogonally layered composition of CLT gives many benefits in terms of structural performance at both in-plane and out-of-plane loading conditions. The layered composition, typically without adhesive bonding at the narrow faces of laminations within the same layer, gives, in combination with the strongly orthotropic material properties of the wood-based laminations, a relatively complex internal force and stress distribution. The element load-bearing capacity is hence not only dependent on the strength properties of the laminations and the dimensions of the element gross cross-section, but also affected by the element lay-up, regarding for example the ratio between longitudinal and transversal layer thicknesses and by the cross-section dimensions of the individual laminations.

A consistent and unified design approach for CLT at pure in-plane shear loading conditions (shear walls) and at in-plane beam loading conditions is missing. For both loading conditions, three shear failure modes need to be considered in the design, see Fig. 1: gross shear failure (mode I), net shear failure (mode II) and shear failure in the crossing areas between adjacent longitudinal and transversal laminations (mode III). A unified test method is also missing where several methods, including “single-node” or “full scale” tests as the so-called Kreuzinger

* Corresponding author.
*E-mail addresses:* henrik.danielsson@construction.lth.se (H. Danielsson), mjelec@gfos.hr (M. Jeleč).

https://doi.org/10.1016/j.conbuildmat.2022.129167
Received 28 May 2022; Received in revised form 31 August 2022; Accepted 11 September 2022
Available online 26 September 2022

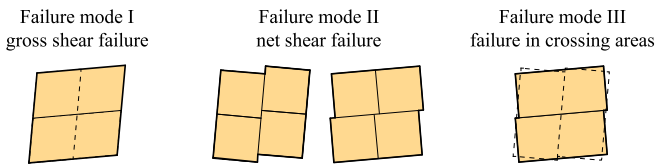


**Fig. 1.** Failure modes at in-plane shear loading.

test method [3], are included in the recently revised European product standard for CLT, see [4,5].

For shear walls, the CLT lay-up is in practice typically such that the external layers are arranged with vertically placed laminations. For pure in-plane shear loading, the layer orientation is however not of importance for prediction of design relevant shear stresses acting in the crossing areas. For beam loading situations, the situation is however slightly different. High bending moment capacity is achieved for a large total width of the layers with laminations oriented in the beam length direction which in practice typically means using horizontally oriented laminations in the external layers. CLT beams with vertical orientation of the lamintations in the external layers would still be relevant for lintels in continuous CLT elements with cut-outs for doors and windows.

Design proposals for in-plane shear loading conditions are so far reported by Bogensperger et al. [6], by Wallner-Novak et al. [7], in ÖNORM B 1995–1-1/A:2018–11 [8] (also included in the draft of the revised version of Eurocode 5) and by Danielsson et al. [9,10]. Design proposals for in-plane beam loading conditions are so far reported by Flaig & Blass [11,12], which are included in the draft of the revised version of Eurocode 5, and by Danielsson & Serrano [13] and Jeleč et al. [14]. Comparisons between full 3D finite element (FE) models and analytical model predictions are presented in [9,10] for pure shear loading conditions and in [14–16] for beam loading conditions. These comparisons indicate significant differences between the analytical models concerning the predicted influence of the CLT element lay-up and predicted maximum shear stresses. Furthermore, compared to FE-results, predictions of models which are included in the draft versions within the ongoing revision of Eurocode 5 show significantly different magnitude and distribution of internal forces and stresses relevant for the determination of load bearing capacity with respect to shear force.

This paper deals with models for the prediction of stress components related to verification of load-bearing capacity of CLT with respect to shear failure mode III – shear failure in the crossing areas constituted by the flatwise bonded areas between laminations of adjacent layers. This failure mode is relevant for both pure in-plane shear loading (shear walls) and at in-plane beam loading conditions. The paper presents a review of previously proposed models for the prediction of shear stresses in crossing areas of CLT for both loading conditions, adopting failure criteria found in the literature without analysing experimental validations. Based on simplifications of models previously presented, a unified design approach that is based on a rational and consistent mechanical background for both loading situations and that shows overall good agreement with FE-results is presented.

## 2. Pure shear loading conditions

### 2.1. Analytical model

Pure in-plane shear loading of CLT (shear walls and diaphragms) and model predictions regarding shear failure mode III is discussed in [9] and [10] and reviewed below. CLT elements without edge-bonding and composed of either 3 layers (CLT 3s), 5 layers (CLT 5s) or seven layers (CLT 7s) are considered and the notation and definitions according to Fig. 2 are used. The individual longitudinal and transversal layers are denoted by index $k$ and the crossing areas are denoted by index $j$, both by acknowledging the element lay-up symmetry with respect to the $z$-direction as illustrated in Fig. 2**b**) for CLT 5s.

At sections (horizontal or vertical) corresponding to locations between adjacent laminations within the same layer, the shear flow $\nu_{xy} = \nu_{yx}$ must be carried by the layers oriented in the direction perpendicular to these sections. The shear flow acting in the $k$ individual layers may be assumed according to

$$\nu_{xy,k} = \beta_{x,k}\nu_{xy} \tag{1}$$

$$\nu_{yx,k} = \beta_{y,k}\nu_{yx} \tag{2}$$

where $\beta_{x,k}$ and $\beta_{y,k}$ are dimensionless weighting factors for the layers with laminations oriented in the $x$- and $y$-directions, respectively.

The weighting factors may be defined from the thickness of the individual layers according to

$$\beta_{x,k} = \frac{t_{x,k}}{t_x} \tag{3}$$

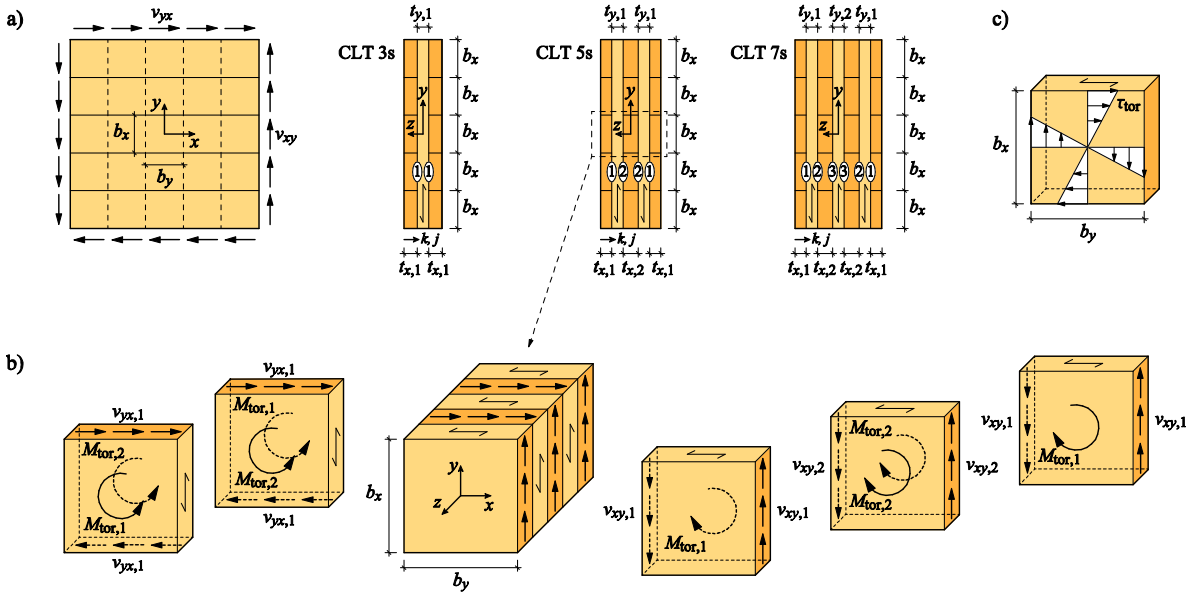


**Fig. 2.** Definition of load and geometry parameters for pure in-plane shear loading.

$$\beta_{y,k} = \frac{t_{y,k}}{t_y} \tag{4}$$

where $t_x = \Sigma t_{x,k}$ and $t_y = \Sigma t_{y,k}$ represent the two net cross-section thicknesses. Other choices of weighting factors are possible, as discussed in [9].

For CLT without edge-bonding of the laminations, the shear flows give rise to torsional moments $M_{\text{tor},j}$ acting in the crossing areas between laminations of adjacent layers, see Fig. 2**b**). The design-relevant torsional shear stress, according to the stress distribution shown in Fig. 2**c**), can be determined according to

$$\tau_{\text{tor},j} = \frac{M_{\text{tor},j}}{I_{\text{P,CA}}} \frac{b_{\max}}{2} \tag{5}$$

where $j = 1$ for CLT 3s, $j = 1$ or 2 for CLT 5s and $j = 1$, 2 or 3 for CLT 7s and where

$$I_{\text{P,CA}} = \frac{b_x b_y}{12}\left(b_x^2 + b_y^2\right) \tag{6}$$

with $b_{\max} = \max(b_x, b_y)$. The stress $\tau_{\text{tor},j}$ represents the maximum value of the shear stress at the centre of the four sides along the perimeter of the crossing area, see Fig. 2**c**).

Based on shear flows according to Eqs. (1) and (2), the torsional moments $M_{\text{tor},j}$ can be determined by equilibrium considerations and the corresponding torsional shear stress components $\tau_{\text{tor},j}$ can be determined from Eq. (5). A general expression for the torsional shear stress in CLT 3s, 5s and 7s may then be formulated as

$$\tau_{\text{tor},j} = \frac{3\nu_{xy}}{b_x} k_{1,j} k_b \tag{7}$$

where the factor $k_{1,j}$ is determined for each crossing area $j$ in width direction according to

$$k_{1,j} = \begin{cases} j = 1\,;\ \{\beta_{x,1}\} & \text{for CLT 3s} \\ j = 1,\ 2\,;\ \left\{\beta_{x,1},\ \dfrac{\beta_{x,2}}{2}\right\} & \text{for CLT 5s} \\ j = 1,\ 2,\ 3\,;\ \left\{\beta_{x,1},\ \beta_{y,1} - \beta_{x,1},\ \dfrac{1}{2} - \beta_{y,1}\right\} & \text{for CLT 7s} \end{cases} \tag{8}$$

with weighting factors $\beta_{x,k}$ and $\beta_{y,k}$ according to Eqs. (3) and (4) and where

$$k_b = \frac{2 b_{\max} b_x}{b_x^2 + b_y^2} \tag{9}$$

which for the special case of equal lamination widths, $b_x = b_y$, gives $k_b = 1.0$.

The maximum value of the torsional shear stress $\tau_{\text{tor,max}}$ in the element width direction is determined according to Eq. (7) by the maximum value of the factor $k_{1,j}$ according to Eq. (8), considering each crossing area $j$. For verification of load-bearing capacity with respect to in-plane shear loading and failure mode III, the torsional shear stress should fulfil the criterion $\tau_{\text{tor,max}} < f_{v,\text{tor}}$ where $f_{v,\text{tor}}$ is a torsional shear strength parameter. This strength parameter can be determined from tests of single crossing areas and making use of Eq. (5) for evaluation of test results. The failure criterion, the involved strength parameter and experimental test results are further discussed in e.g. [5,16–18]. For tests on European softwood laminations and loading of single crossing areas in pure torsion, mean torsional shear strengths of $f_{v,\text{tor,mean}} \approx 3.5$ MPa are reported in [19–21] and a characteristic value of $f_{v,\text{tor,k}} = 2.5$ MPa is proposed in background documents for the revision of Eurocode 5.

### 2.2. Comparison of model predictions and discussion

Comparisons between results according to full 3D FE-models and the analytical model predictions are presented in [9] for CLT 3s and 5s and in [10] for CLT 7s, considering symmetric element lay-ups and equal width of all laminations (i.e. $b_x = b_y = b$). Four analytical models were considered, as follows; Model A – Representative Volume Sub-Element (RVSE) approach according to Bogensperger et al. [6], Model B – the approach stated by Wallner-Novak et al. [7], Model C – the approach stated in ÖNORM B 1995–1-1/A:2018–11 [8] and in the draft version of the revised version of Eurocode 5 (CEN/TC 250/SC5) [22] and model D – reviewed above in Section 2.1. The FE-models were composed of five longitudinal and five transversal laminations in each layer (see Fig. 2**a**) and considered symmetry in the out-of plane direction. The laminations were modelled as 3D solids with orthotropic linear elastic behaviour and the flatwise bonding between the laminations was modelled by a contact formulation. Loading was applied as shear forces on the end-faces of the respective laminations and displacement boundary conditions where applied to prevent rigid body movements.

The evaluation of results was based on consideration of average lamination shear flows $\nu_{xy,k}$ and $\nu_{yx,k}$ for individual laminations and crossing area torsional moments $M_{\text{tor},j}$ at the centremost part of the model (see Fig. 2), by integration of stresses over the considered laminations' cross-sections and crossing areas, respectively. For comparison to analytical model predictions, values of the torsional shear stress $\tau_{\text{tor},j}$ according to Eq. (5) were determined based on the numerically found values of $M_{\text{tor},j}$.

Comparisons of model predictions for the maximum torsional shear stress, considering different CLT element lay-ups, are presented in Fig. 3 based on results presented in [9,10]. These results are based on lamination widths $b_x = b_y = 150$ mm, with element gross cross-section thickness ($t_{\text{gross}}$) and shear loading ($v_{xy}$) as; 100 mm and 100 N/mm for CLT 3s, 200 mm and 200 N/mm for CLT 5s and 240 mm and 240 N/mm for CLT 7s.

For CLT 3s, weighting factors $\beta_{x,k}$ according to Eq. (3) are (due to symmetry) always accurate and results of the FE-analyses are in very close agreement with model D for all considered lay-ups, which is also the case for models A and B. Model C predicts maximum torsional shear stresses in agreement with the numerical results only within the range $1.0 \le t_x/t_y \le 2.0$, see Fig. 3. It is concluded in [9] that the maximum torsional shear stress found from FE-analyses for CLT 3s is unaffected by the maximum layer thickness $t_{\max} = \max(t_{x,k}, t_{y,k})$ and also unaffected by the lay-up in terms of the ratio between the total longitudinal and transversal layer thicknesses $t_x/t_y$.

For CLT 5s and 7s, models A, B, C and D show significant differences concerning the predicted influence of the CLT element lay-up and predicted maximum torsional stresses, see Fig. 3**.** None of the analytical models give predictions in full agreement with the FE-results for the complete range of considered lay-ups. For model D, the differences between numerical and analytical predictions regarding the maximum torsional stress are due to differences in the predictions of the shear flows $\nu_{xy,k}$ and $\nu_{yx,k}$ and assumed weighting factors $\beta_{x,k}$ and $\beta_{y,k}$ within the respective layers in the element width direction. Such differences are illustrated for CLT 5s in Fig. 3 by introducing two alternatives for the weighting factors $\beta_{x,k}$ for model D, i.e. defining $\beta_{x,k}$ based on either the individual layer thicknesses according to Eq. (3) or based on adjustments to results from FE-analyses for beam loading conditions, as described in Section 3.2 below and according to Eq. (20). Presented results indicate very close agreement between FE-results and the two alternatives of model D for specific lay-ups with $t_{x,2}/t_{x,1} = 2.0$, i.e. for an internal longitudinal layer thickness twice the external longitudinal layer thicknesses, where for other lay-ups, some discrepancies between the results are found. Such lay-up for CLT 5s, and for CLT 7s with the addition of a fixed ratio $t_{y,2}/t_{y,1} = 1.0$, seems to be the most favourable lay-up according to FE-results and Model D, since these lay-ups give equal torsional moments for all crossing areas in the element width direction and yield the lowest possible value of the torsional shear stresses.

Based on the FE-results presented in [9] and [10] it was concluded that maximum torsional stress is unaffected by the lay-up in terms of the

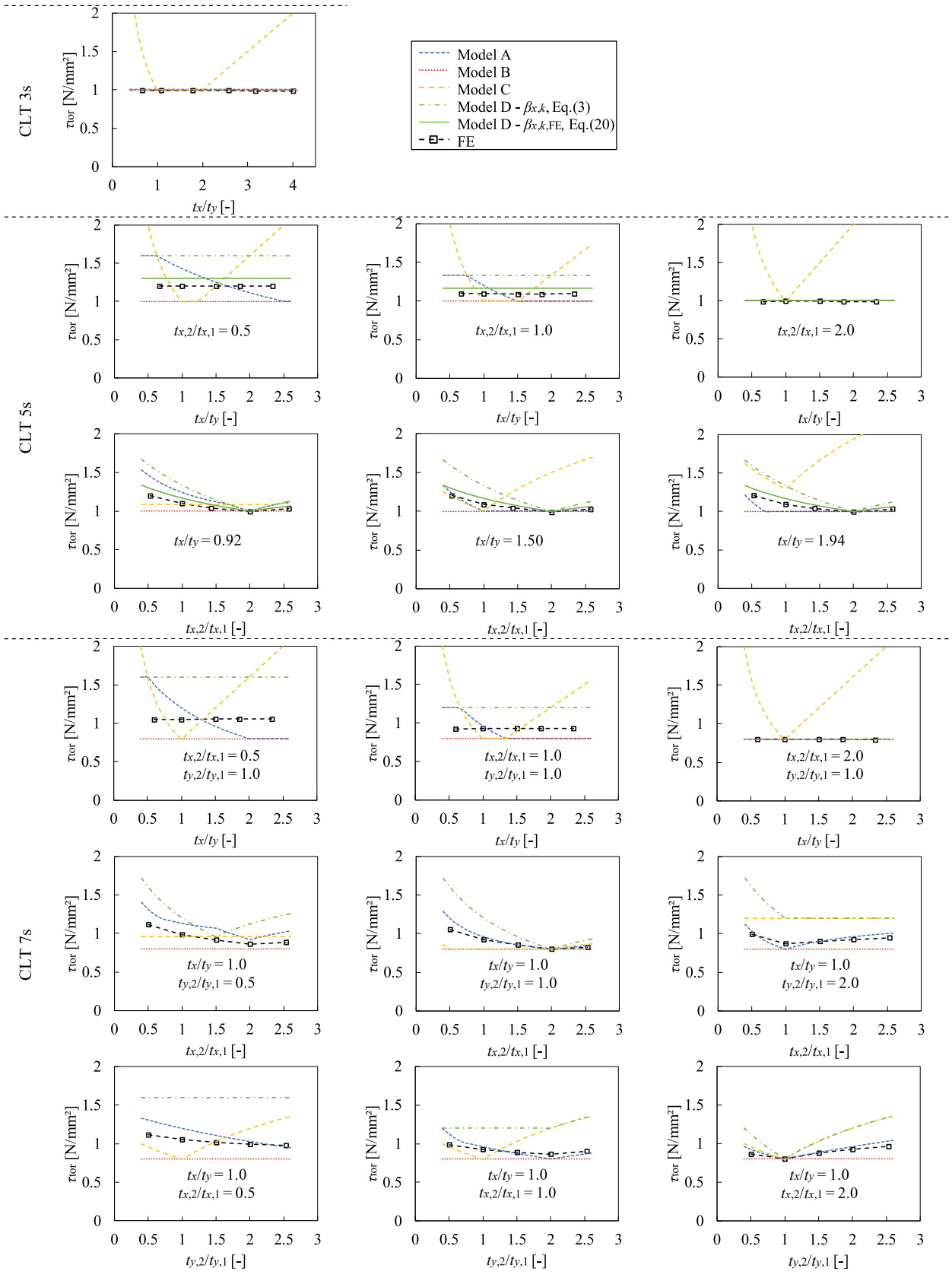


**Fig. 3.** Comparison of maximum torsional shear stress for CLT 3s, 5s and 7s according to FE analysis and analytical models A-D for pure shear loading conditions.

ratio between the total longitudinal and transversal layer thicknesses, $t_x/t_y$, for fixed ratios between the respective individual longitudinal and transversal layer thicknesses, see Fig. 3, i.e. for constant ratio $t_{x,2}/t_{x,1}$ for CLT 5s and constant ratios $t_{x,2}/t_{x,1}$ and $t_{y,2}/t_{y,1}$ for CLT 7s.

Model D with weighting factors $\beta_{x,k}$ according to Eq. (3) gives stress predictions for CLT 5s and 7s either in agreement with results of the FE-analysis or higher (conservative) compared to the FE-analysis, see Fig. 3. Although model D is not in perfect agreement with the results of FE-analysis, among the models presented in [9] and [10], it is the only one that has the same basic behaviour as that predicted by the FE-analyses both as regards the influence of the ratio between the longitudinal and transversal layer thicknesses, $t_{x,2}/t_{x,1}$ and $t_{y,2}/t_{y,1}$, and as regards the influence of the ratio of the two net cross-section thicknesses, $t_x/t_y$. It is hence concluded that model D, presented in [9,10] and reviewed in Section 2.1, with weighting factors $\beta_{x,k}$ and $\beta_{y,k}$ according to Eqs. (3) and (4), respectively, could be considered to be a reasonable choice for practical design purposes and for use in structural design codes.

## 3. Beam loading conditions

### 3.1. Analytical model

The internal force distribution differs between the cases of pure in-plane shear loading and in-plane beam loading conditions. For beam loading conditions, see Fig. 4, uniaxial shear stresses acting over the crossing areas in the $x$- and $y$-directions are present in addition to the torsional shear stress discussed above for the case of pure in-plane shear loading.

The presentation below considers beams having an integer number $m = h/b_x$ of longitudinally oriented laminations and the element orientation is such that these are placed in the external layers, a layer orientation which is here denoted beam orientation $L$. Index $i$ refers to the position of the laminations in the beam height ($y$) direction, index $k$ refers to the position of the layers in the beam width direction and index $j$ refers to the position of the crossing areas in the beam width direction. Elements with symmetric lay-up in the beam width direction are considered, which is also acknowledged in the notation for indices $k$ and $j$.

The beam bending is assumed to give a linear normal strain distribution in the beam height direction. Considering elements without edge-bonding and considering the low stiffness of the laminations in the direction perpendicular to grain compared to the direction parallel to grain, normal stress parallel to the beam axis, $\sigma_x$, is assumed to be present only in the layers with laminations having grain direction oriented along the $x$-axis. Assuming equal parallel to grain stiffness for these laminations gives a normal stress $\sigma_x$ which is constant with respect to the beam width direction. Shear stresses $\tau_{xy}$ are further present in all layers but since elements without edge-bonding are considered, all narrow faces of the laminations are assumed to be traction-free.

The beam loading case give rise to shear stresses ($\tau_{zx}$ and $\tau_{zy}$) acting in the crossing areas. These can be decomposed into stresses due to three basic in-plane loading situations: (a) shear stress parallel to the beam axis, (b) shear stress perpendicular to the beam axis and (c) torsional shear stress $\tau_{\text{tor}}$. The corresponding resulting forces $F_{x,i,j}$ and $F_{y,i,j}$ and the resulting torsional moment $M_{\text{tor},i,j}$ are illustrated in Fig. 4 which also includes illustrations of the assumed shear stress distribution according to the model by Flaig & Blass, see [11,12,23–26]. The forces and the torsional moment acting over an individual crossing area $i$, $j$ can be determined from static equilibrium, considering the cross-sectional forces and moments acting in the corresponding lamination oriented along the $x$-axis, see [13,27].

For verification of load-bearing capacity with respect to shear failure mode III, failure criteria may be formulated from the three crossing area shear stress components illustrated in Fig. 4. The uniaxial shear stress in the direction perpendicular to the beam axis, $\tau_{zy}$, should be relevant mostly in areas of high concentrated loads in the direction perpendicular to the beam axis (e.g. at short supports or local load introductions) and should, in general, be of less importance compared to the uniaxial shear stress component in the direction parallel to the beam axis. Considering beam orientation $L$ and disregarding the shear stress component $\tau_{zy}$, a failure criterion considering linear interaction between the two remaining shear stress components is in [12] and [23] suggested according to

$$\frac{\tau_{\text{tor}}}{f_{v,\text{tor}}} + \frac{\tau_{zx}}{f_r} \leq 1.0 \tag{10}$$

where $f_{v,\text{tor}}$ is the torsional shear strength parameter (see Section 2) and where $f_r$ is the strength at pure uniaxial shear loading over the crossing area, corresponding to pure rolling shear stress. Experimental test results of single crossing areas as compiled in [17] and [27] suggest a mean rolling shear strength $f_{r,\text{mean}} \approx 1.5$ MPa and a mean torsional shear strength $f_{v,\text{tor,mean}} \approx 3.5$ MPa for European softwood species.

Forces $F_{x,i,\ j}$ acting in the crossing areas between laminations of

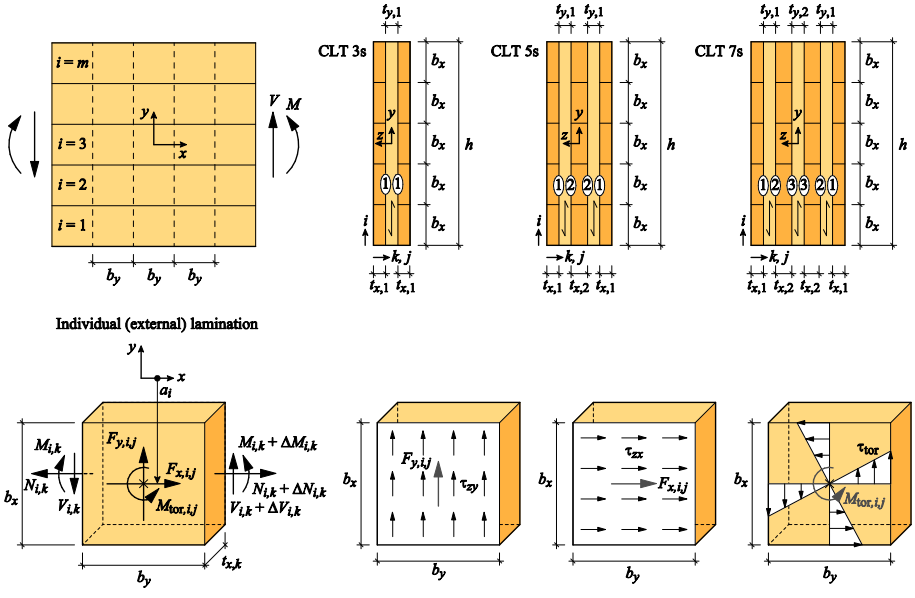


**Fig. 4.** Illustration of beam model and definition of load and geometry parameters.

adjacent layers appear due to the differential lamination normal force $\Delta N_{i,k}$, caused by a differential bending moment $\Delta M$ and presence of a shear force $V$. The linear distribution of normal strain and stress in the longitudinal laminations, due to bending of the beam, yields forces $F_{x,i,j}$ which vary linearly with the distance $a_i$ between the beam centre-line ($y = 0$) and the centre line of the considered lamination $i$

$$a_i = b_x\left|\frac{m+1}{2} - i\right| \tag{11}$$

The magnitude of the forces $F_{x,i,j}$ can be found from static equilibrium and can according to [13,17,27,28] for CLT 3s, 5s and 7s with beam orientation $L$ be expressed as

$$F_{x,i,j} = \frac{12V}{h^3}\frac{1}{n_{\mathrm{CA},k}}\frac{t_{x,k}}{t_x}b_x b_y a_i \tag{12}$$

where $j = k = 1$ for CLT 3s, $j = k = 1$ or 2 for CLT 5s and where for CLT 7s, the cases $j = k = 1$ or 2 and $j = 3$, $k = 2$ are considered. Further, $n_{\mathrm{CA},k}$ is the number of crossing areas that the individual longitudinal lamination $k$ shares with adjacent transversal laminations, i.e. $n_{\mathrm{CA},k} = 1$ for external ($k = 1$) or $n_{\mathrm{CA},k} = 2$ for internal ($k = 2$) longitudinal laminations, respectively, see Fig. 4. For CLT 7s, the equality $F_{x,i,2} = F_{x,i,3}$ is derived from symmetry considerations and the assumption of a uniformly distributed parallel to grain normal stress distribution in the beam width direction. The expression given in Eq. (12) corresponds to the model presented by Flaig in [23] for CLT 3s and 5s. The design equations suggested by Flaig in [23] and by Flaig & Blass in [12] are however based on simplification by disregarding the influence of the individual layer thicknesses and assuming $(1/n_{\mathrm{CA},k})\bullet(t_{x,k}/t_x)$ to be constant for all layers.

By assuming a uniform shear stress distribution over the respective crossing areas as illustrated in Fig. 4, the shear stress component $\tau_{zx,i,j}$ is given by

$$\tau_{zx,i,j} = \frac{F_{x,i,j}}{b_x b_y} \tag{13}$$

which by the use of $F_{x,i,j}$ according to Eq. (12) for CLT 3s, 5s and 7s yields

$$\tau_{zx,i,j} = \frac{12V}{h^3}\frac{1}{n_{\mathrm{CA},k}}\frac{t_{x,k}}{t_x}a_i \tag{14}$$

where $j$, $k$ and $n_{\mathrm{CA},k}$ should be used as for Eq. (12).

At locations in the $x$-direction corresponding to sections in-between adjacent laminations oriented in the $y$-direction, the shear force $V$ must be carried solely by the laminations oriented in the $x$-direction, i.e. the longitudinal laminations. The distribution of the total shear force $V$ over the individual longitudinal laminations can for these locations be expressed as

$$V_{i,k} = \alpha_i \beta_{x,k} V \tag{15}$$

where $\alpha_i$ and $\beta_{x,k}$ are dimensionless weighting factors describing the distribution of the shear force in the beam height ($\alpha_i$) and the beam width ($\beta_{x,k}$) directions, respectively. Weighting factors $\alpha_i$ according to

$$\alpha_i = \frac{6i - 6i^2 + m(6i-3) - 2}{m^3} \tag{16}$$

are proposed in [13], based on the parabolic shear stress distribution found from conventional engineering beam theory for a homogeneous beam composed of $m$ laminations in the beam height direction, with equal lamination width $b_x = h/m$. Weighting factors $\beta_{x,k}$ describing the shear force distribution in the beam width direction based on the individual longitudinal layer thicknesses as defined in Eq. (3) is further outlined in [15].

The individual lamination shear forces $V_{i,k}$ are of importance in relation to the stress state in the crossing areas and thus for design with respect to shear failure mode III, since they influence the torsional moments $M_{\mathrm{tor},i,j}$ and consequently the torsional shear stresses $\tau_{\mathrm{tor},i,j}$. The crossing area torsional moments can be found from static equilibrium considering the differential lamination shear forces $\Delta V_{i,k}$ and the differential lamination bending moment $\Delta M_{i,k}$.

The torsional moment $M_{\mathrm{tor},i,j}$ may for CLT 3s, 5s and 7s with beam orientation $L$, according to [13,17,27,28], be formulated in a consistent manner as

$$M_{\mathrm{tor},i,j} = Vb_y\left(\alpha_i k_{1,j} - \frac{1}{n_{\mathrm{CA},k}}\frac{t_{x,k}}{t_x}\frac{b_x^3}{h^3}\right) \tag{17}$$

where $j$, $k$ and $n_{\mathrm{CA},k}$ should be used as for Eq. (12). The factor $k_{1,j}$ is the same as found also for pure shear loading conditions, see Section 2.1, which should be calculated according to Eq. (8) for each crossing area $j$ in the width direction considering corresponding weighting factors $\beta_{x,k}$ and $\beta_{y,k}$ according to Eqs. (3) and (4). Eq. (17) is, however, slightly reformulated compared to equations presented in [13,17,27,28], where instead of weighting factors $\beta_{x,k}$, a more general form with the factor $k_{1,j}$ is used to allow for a consistent formulation for CLT 3s, 5s and 7s.

The maximum torsional stress for crossing area $i$, $j$ according to the stress distribution as illustrated in Fig. 4 is then found as

$$\tau_{\mathrm{tor},i,j} = \frac{M_{\mathrm{tor},i,j}}{I_{\mathrm{P,CA}}}\frac{b_{\max}}{2} \tag{18}$$

which by the use of $M_{\mathrm{tor},i,j}$ according to Eq. (17) for CLT 3s, 5s and 7s yields

$$\tau_{\mathrm{tor},i,j} = \frac{3V}{b_x^2}\left(\alpha_i k_{1,j} - \frac{1}{n_{\mathrm{CA},k}}\frac{t_{x,k}}{t_x}\frac{b_x^3}{h^3}\right)k_b \tag{19}$$

where $j$, $k$ and $n_{\mathrm{CA},k}$ should be used as in Eq. (12) and with $k_{1,j}$ and $k_b$ according to Eqs. (8) and (9), respectively.

According to the above given equations, the parallel to beam axis uniaxial shear stress $\tau_{zx,i,j}$ (which is assumed to be constant within an individual crossing area) varies linearly between the different crossing areas in the beam height direction. The maximum value of $\tau_{zx,i,j}$ is found at the lowermost ($i = 1$) and uppermost ($i = m$) crossing area, with the minimum at the beam centre-line. The torsional moments $M_{\mathrm{tor},i,j}$, and hence the torsional shear stress $\tau_{\mathrm{tor},i,j}$, also varies over the beam height direction but instead with the maximum values found at the centremost crossing area and minimum values at the upper- and lowermost crossing areas.

### 3.2. Comparison of model predictions and discussion

Comparisons between results according to full 3D FE-models and analytical model predictions regarding lamination shear forces $V_{i,k}$, parallel to beam axis forces $F_{x,i,j}$ and torsional moments $M_{\mathrm{tor},i,j}$ are presented in [14,15,27] for CLT 3s and 5s and in [27] for CLT 7s considering beam orientation $L$. Two analytical models were considered, as follows, Model A – the approach stated by Blass & Flaig [11,12] and Flaig [23,26] and found in the draft version of the revised version of Eurocode 5 (CEN/TC 250/SC5) [22] and Model B – reviewed above in Section 3.1. Beams with $m = 3$, 4, 5 and 6 longitudinal laminations in the beam height direction and a wide range of element lay-ups regarding the ratio between internal and external longitudinal layer thicknesses were considered for CLT 5s ($0.31 \le t_{x,2}/t_{x,1} \le 2.6$) and for CLT 7s ($0.33 \le t_{x,2}/t_{x,1} \le 2.0$) with a fixed ratio between internal and external transversal layer thicknesses $t_{y,2}/t_{y,1} = 1.0$. The FE-models were based on assumptions of linear elastic behaviour and in principle formulated and evaluated as described in Section 2.2 (for the case of pure in-plane shear loading), however with loads adapted according to the beam loading situation illustrated in Fig. 4.

The distribution in the beam width direction of shear forces $V_{i,k}$, torsional moments $M_{\mathrm{tor},i,j}$ and parallel to beam axis shear forces $F_{x,i,j}$ are

(due to symmetry) accurately predicted by model B and weighting factors $\beta_{x,k}$ according to Eq. (3) for all lay-ups considering CLT 3s. The comparisons between FE-results and analytical model predictions hence showed overall very good agreement in this respect. Also, the distribution of forces/moments in the beam height ($y$) direction agreed very well between the numerical results and analytical model B for CLT 3s, indicating that the factors $\alpha_i$ according to Eq. (16) represent the distribution of shear forces $V_{i,k}$ in the beam height direction accurately, see Fig. 5.

The comparisons presented in [14,15,27] for CLT 5s and in [27] for CLT 7s also revealed very good agreement in terms of distributions of forces and torsional moments between the laminations and crossing areas in the beam height ($y$) direction for all considered beam geometries, see Fig. 4. For this comparison, only the distributions of the total forces (absolute values) for each location $i$ in the beam height direction were considered, i.e. shear forces $V_i$, axial shear forces $F_{x,i}$ and torsional moments $M_{\text{tor},i}$ and not the forces/moments in an individual lamination and an individual crossing area ($V_{i,k}$, $F_{x,i,j}$ and $M_{\text{tor},i,j}$).

The (implicit) assumption of equal lamination shear forces and the (explicit) assumption of equal torsional moments for all crossing areas in the beam height direction according to analytical model A are clearly in disagreement with the results of the FE-analyses and predictions of model B.

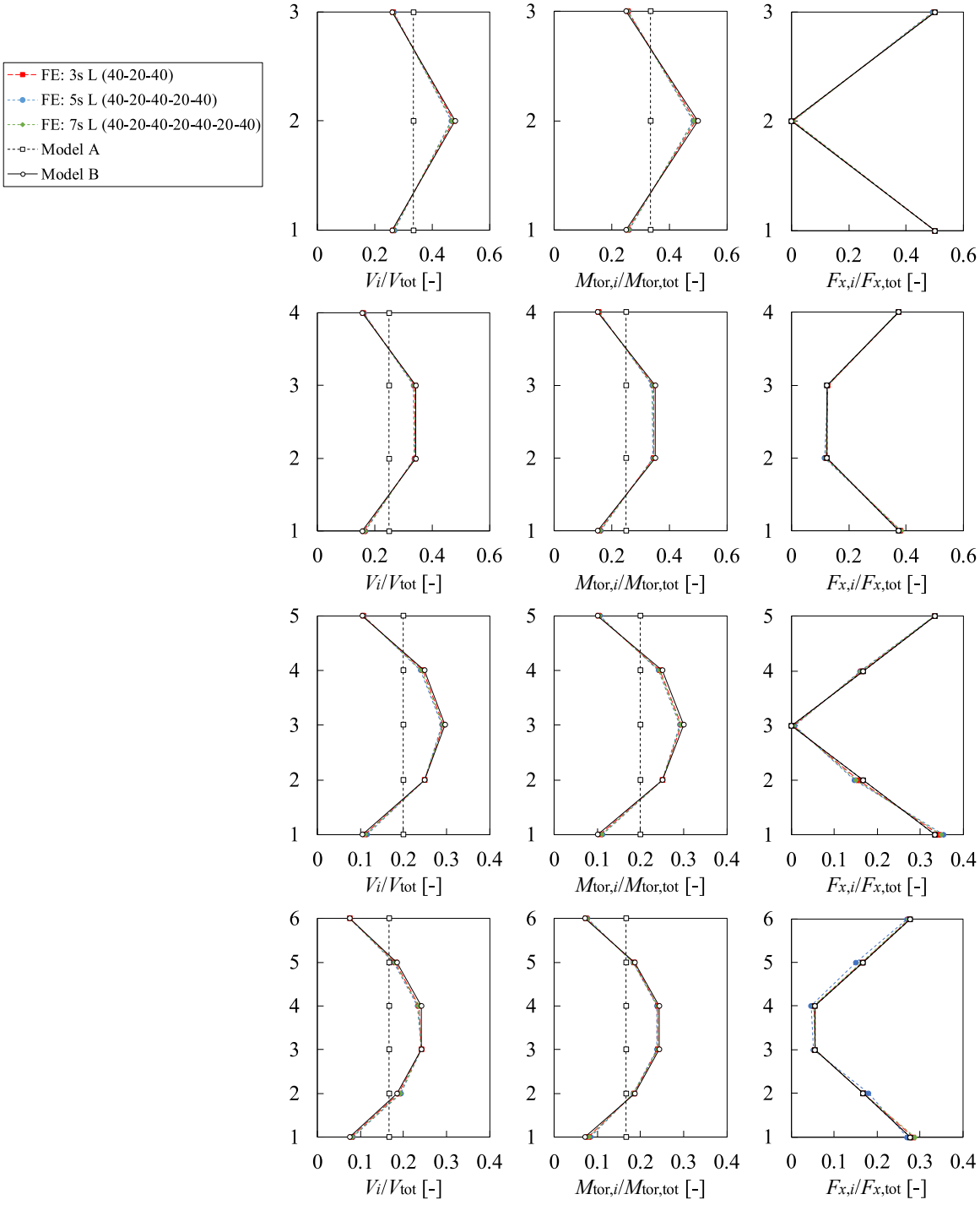


**Fig. 5.** Distribution in beam height direction of internal forces and moments according to FE-analyses and analytical models for CLT 3s, 5s and 7s with $3 \leq m \leq 6$ longitudinal laminations in the beam height direction.

The FE-results presented in [14,15,27] concerning the parallel to beam axis shear forces $F_{x,i,j}$ and their distribution in the beam width direction showed good agreement with predictions according to model B for all crossing areas and all considered element lay-ups, see Fig. 6. The FE-results concerning lamination shear forces $V_{i,k}$ and torsional moments $M_{\text{tor},i,j}$ were accurately predicted by model B considering weighting factors $\beta_{x,k}$ according to Eq. (3) for lay-ups with an internal longitudinal layer thickness twice the external longitudinal layer thickness, i.e. $t_{x,2}/t_{x,1} = 2.0$, see Fig. 6. For this comparison, only the distributions in the beam width direction of the total forces (absolute values) for each longitudinal layer $k$ and corresponding crossing area $j$ were considered, i.e. shear forces $V_k$, axial shear forces $F_{x,j}$ and torsional moments $M_{\text{tor},j}$ and not the forces/moments in an individual lamination and an individual crossing area ($V_{i,k}$, $F_{x,i,j}$ and $M_{\text{tor},i,j}$).

For lay-ups with $t_{x,2}/t_{x,1} < 2.0$, the analytical model B predicts greater shear forces $V_{i,k}$ for the external longitudinal layers ($k = 1$) compared to the FE-model predictions and consequently also predicts greater values of the maximum torsional moments, which for these lay-ups are found in the outermost crossing area ($j = 1$). Compared to FE-results, the analytical model B overestimates the maximum torsional shear stress for CLT lay-ups typically used in practice, with $t_{x,2}/t_{x,1} < 2.0$. For the special case $t_{x,2}/t_{x,1} = 2.0$, very good agreement is found between analytical model predictions and FE-results for all considered lay-ups, also in terms of the number of laminations in the beam height

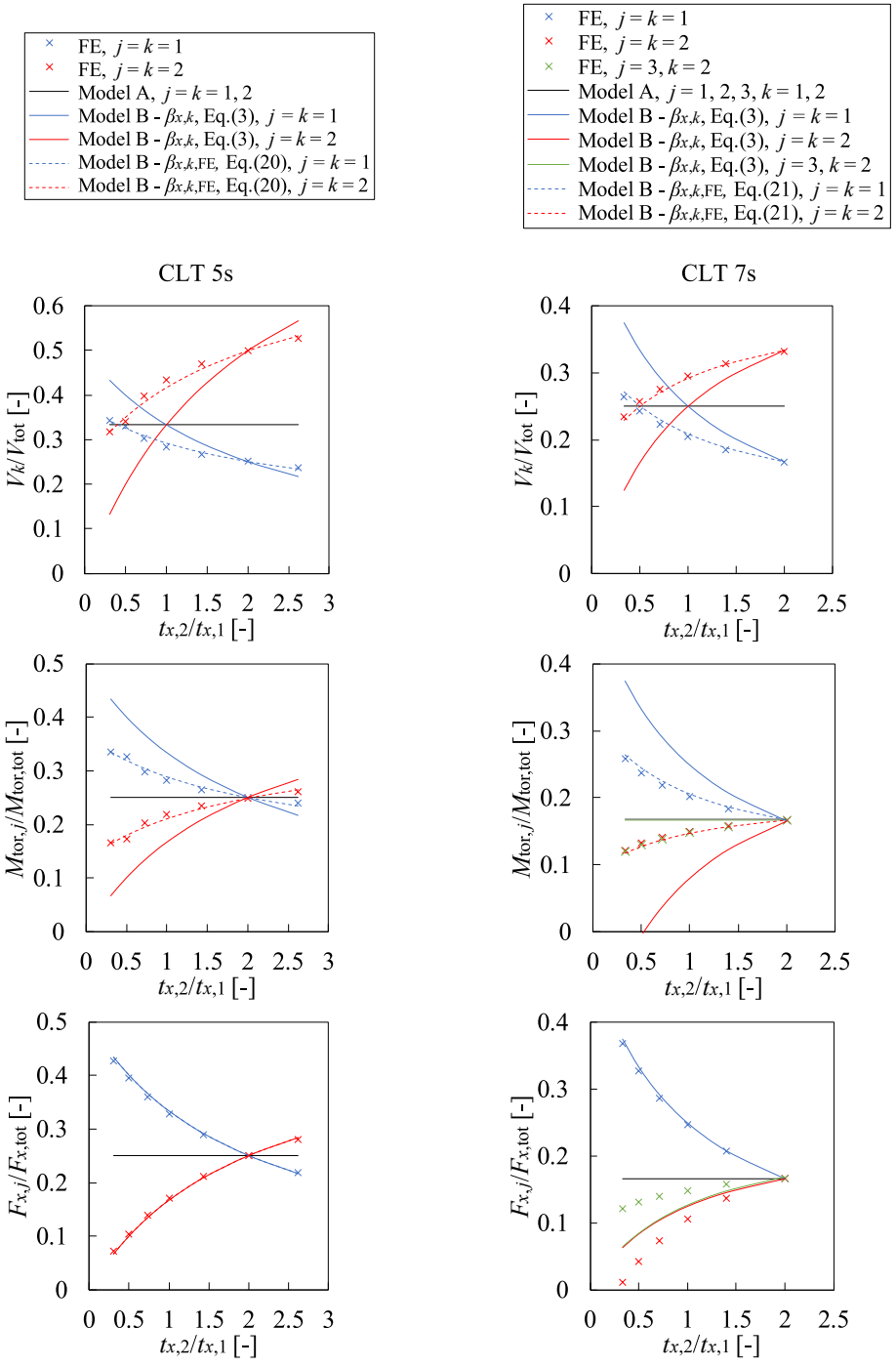


**Fig. 6.** Distribution in beam width direction of internal forces and moments according to FE-analyses and analytical models for varing lay-ups $0.31 \leq t_{x,2}/t_{x,1} \leq 2.6$ of CLT 5s and $0.33 \leq t_{x,2}/t_{x,1} \leq 2.0$ with $t_{y,2}/t_{y,1} = 1.0$ of CLT 7s.

direction. On the contrary, the assumptions of equal torsional moments and equal axial shear forces for all crossing areas in the beam width direction according to analytical model A, irrespective of the considered lay-ups, are clearly in disagreement with the results of the FE-analyses (and predictions of model B). The study concerning lamination placement and varying widths $b_x$ of the individual longitudinal laminations within a single CLT beam presented in [17,27] for CLT 3s and 5s and in [27,28] for CLT 7s revealed similar results as discussed above for the assumption of equal laminations widths.

The comparisons between analytical model predictions and FE-results reviewed above revealed some deviations regarding forces and moments acting in individual laminations and crossing areas. These deviations are related to the distribution of laminations shear forces $V_{i,k}$ in the beam width direction, which also govern the distribution of torsional moments acting in the crossing areas between laminations of adjacent layers. The FE-analyses gave results with a more uniform distribution of shear forces $V_{i,k}$ in the beam width direction compared to model B with predictions using $\beta_{x,k}$ according to Eq. (3). Based on manual curve-fitting regarding the influence of the individual layers' thicknesses on the distribution of the lamination shear forces $V_{i,k}$ found from FE-analyses of CLT 5s and 7s beams with orientation $L$ as presented in [14,15,27] and [27,28], respectively, adjusted expressions for the weighting factors $\beta_{x,k}$ were determined. Overall good agreement between FE-results and model B predictions of lamination shear forces and maximum torsional moments were found for weighting factors

$$\beta_{x,k,\mathrm{FE}} = \begin{cases} \frac{1}{8}\left(1 + 4\frac{t_{x,k}}{t_x}\right) & \text{for } k = 1 \\ \frac{1}{4}\left(1 + 2\frac{t_{x,k}}{t_x}\right) & \text{for } k = 2 \end{cases} \tag{20}$$

for CLT 5s and for weighting factors

$$\beta_{x,k,\mathrm{FE}} = \begin{cases} \frac{1}{6}\left(0.5 + 3\frac{t_{x,k}}{t_x}\right) & \text{for } k = 1 \\ \frac{1}{6}\left(1 + 3\frac{t_{x,k}}{t_x}\right) & \text{for } k = 2 \end{cases} \tag{21}$$

for CLT 7s, see Fig. 6.

The FE-results presented in [27] for CLT 7s indicate some differences between axial shear forces $F_{x,i,j}$ and equality of torsional moments $M_{\mathrm{tor},i,j}$ for $j = 2$ and 3 for all considered lay-ups, see Fig. 6. On contrary, for $j = 2$ and 3 analytical model B assumes equal axial shear forces $F_{x,i,j}$ and different torsional moments $M_{\mathrm{tor},i,j}$ according to Eq. (12) and Eq. (17), respectively. Equal torsional moments $M_{\mathrm{tor},i,j}$ for $j = 2$ and 3 according to Eq. (17) are obtained just for the specific case with an internal longitudinal layer thickness twice the external longitudinal layer thickness, $t_{x,2}/t_{x,1} = 2.0$, and equal transversal layer thicknesses, $t_{y,2}/t_{y,1} = 1.0$, see Fig. 6. Such a lay-up seems also to be the most favourable lay-up according to FE-results and Model B, as was the case of pure shear loading conditions, see Section 2.2, i.e. the lay-up giving equal torsional moments for all crossing areas ($j$ = 1, 2 and 3) in the element width direction and yielding the lowest possible value of the torsional shear stresses. Adjusted expressions for the weighting factors $\beta_{x,k,\mathrm{FE}}$ according to Eq. (21) were derived in accordance with results of FE-analysis assuming equal torsional moments $M_{\mathrm{tor},i,j}$ for $j$ = 2 and 3 for all considered lay-ups. Only two crossing areas need then to be considered for CLT 7s ($j = k = 1$ or 2), meaning that $\beta_{x,k,\mathrm{FE}}$ and $n_{\mathrm{CA},k}$ may be used in Eqs. (17) and (19) instead of the factor $k_{1,j}$.

### 3.3. Design relevant stresses and critical crossing areas

The maximum value of the parallel to beam axis shear stress, $\tau_{zx,i,j}$, and the maximum value of the torsional shear stress, $\tau_{\mathrm{tor},i,j}$, are in general not found within the same crossing area, considering the beam height direction. This complicates the procedure of verification of load-bearing capacity since, in general, all $m$ crossing areas in the beam height direction would need to be considered in the design. As stated in Section 3.1, the maximum torsional shear stress is found at the centre of the beam, with respect to the beam height direction. For the parallel to beam axis shear stress, minimum values are found at the beam centre-line while the maximum stress is found in the upper/lower-most crossing areas.

Considering the proposed failure criterion according to Eq. (10) and assuming a strength ratio $f_{v,\mathrm{tor}}/f_r = 3.5/1.5 \approx 2.3$, it has in previous publications (see [13,14,17,27,28]) been shown that the critical crossing area is located close to the beam centre-line (the neutral axis), for the here considered numerical and analytical models. By critical crossing area is here meant the crossing area which shows the highest utilisation ratio according to the failure criterion in Eq. (10). For a critical crossing area with placement close to the neutral axis of the beam, a (conservative) choice is to assume $a_i = b_x/2$ in Eq. (14) for calculation of $\tau_{zx,i,j}$, which corresponds to the maximum possible distance between the beam centre-line and the centre-line of the most centrically placed longitudinal lamination. For CLT 3s, 5s and 7s, this simplification yields a design relevant parallel to beam axis shear stress according to

$$\tau_{zx,\,j} = \frac{6V}{h^3}\frac{b_x}{n_{\mathrm{CA},k}}\frac{t_{x,k}}{t_x} \tag{22}$$

where $j$, $k$ and $n_{\mathrm{CA},k}$ should be used as in Eq. (12).

By identification of the most centrically placed crossing area as the critical crossing area, several simplifications regarding predictions of the design relevant torsional shear stress $\tau_{\mathrm{tor,max}}$ are possible. To arrive at convenient design equations, two simplifications are introduced here. The first of these two simplifications relates to the distribution of lamination shear forces $V_{i,k}$ in the beam width direction and the corresponding weighting factors $\beta_{x,k}$, see Eq. (15). The second simplification relates to the distribution of the shear forces $V_{i,k}$ in the beam height direction and the corresponding weighting factors $\alpha_i$, see Eqs. (15) and (16). The maximum torsional shear stress is given by the maximum value of $\alpha_i$ which in turn depends on the total number of laminations $m$ in the beam height direction, where $m = h/b_x$. Approximations according to

$$\alpha_{\mathrm{max,approx},1} = \frac{3}{2}\frac{1}{m} - \frac{4}{2}\frac{1}{m^3} \tag{23}$$

$$\alpha_{\mathrm{max,approx},2} = \frac{3}{2}\frac{1}{m} - \frac{1}{2}\frac{1}{m^3} \tag{24}$$

are proposed in [14]. Compared to Eq. (16), $\alpha_{\mathrm{max,approx},1}$ gives exact values for even number $m$ laminations while $\alpha_{\mathrm{max,approx},2}$ gives exact values for odd number $m$ laminations. Approximation according to $\alpha_{\mathrm{max,approx},1}$ and $\alpha_{\mathrm{max,approx},2}$ gives for $m \geq 4$ no more than 5 % and 7 % error compared to the exact maximum value of $\alpha_i$ according to Eq. (16). To allow for a more uniform formulation for CLT 3s, 5s and 7s, further simplifications for max($\alpha_i$) may be introduced according to

$$\alpha_{\mathrm{max,approx},3} = \frac{3}{2}\frac{1}{m} \tag{25}$$

which for $m \geq 3$ gives no more than 9 % error compared to the exact value. Ratios between the three approximations and the exact value of max($\alpha_i$) are presented in Fig. 7.

By the introduction of the simplifications mentioned above, two different suggestions for expressions for the design-relevant torsional shear stress, based on adjustments to FE-results, are discussed in [14,17,27,28] for CLT 3s, 5s and in [27,28] for CLT 7s with beam orientation $L$. These suggestions can be formulated as follows

$$\tau_{\mathrm{tor},\,j} = \frac{3V}{b_x^2}\frac{1}{n_{\mathrm{CA},k}}\left(\alpha_{\mathrm{max,approx},1}\beta_{k,x,\mathrm{FE}} - \frac{t_{x,k}}{t_x}\frac{b_x^3}{h^3}\right)k_b \tag{26}$$

and

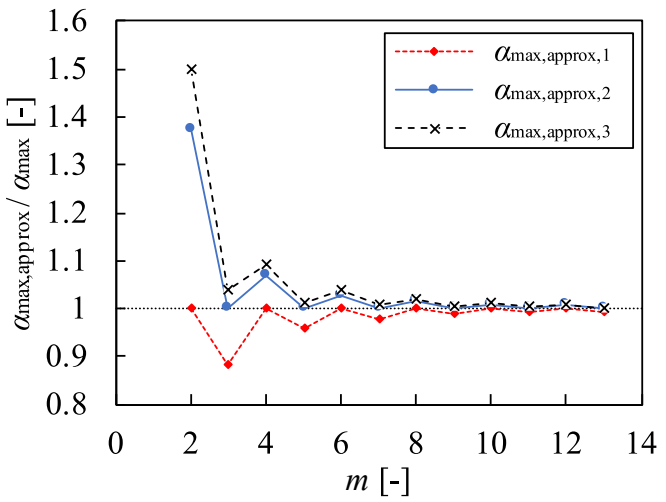


**Fig. 7.** Ratios of approximate values and exact values of max ($\alpha_i$).

$$\tau_{\text{tor},j} = \frac{3V}{b_x^2}\frac{1}{n_{\text{CA},k}}\frac{t_{x,k}}{t_x}\left(\frac{b_x}{h} - \frac{b_x^3}{h^3}\right)k_b\gamma \tag{27}$$

with

$$\gamma = \begin{cases} \frac{3}{2} & \text{for CLT 3s} \\ 0.20\frac{t_{x,2}}{t_{x,1}} + 1.1 & \text{for CLT 5s} \\ 0.25\frac{t_{x,2}}{t_{x,1}} + 1.0 & \text{for CLT 7s} \end{cases} \tag{28}$$

where $j$, $k$ and $n_{\text{CA},k}$ should be used as in Eq. (12). The factor $k_b$ is given by Eq. (9) and weighting factors $\beta_{x,k,\text{FE}}$ in Eq. (26) are given by Eqs. (20) and (21) for CLT 5s and 7s, respectively, while for CLT 3s due to symmetry $\beta_{x,k,\text{FE}} = t_{x,k}/t_x = 0.5$ for all lay-ups.

To allow for more uniform and simplified formulations for CLT 3s, 5s and 7s, a further conservative assumption may be introduced in Eq. (27) with $\gamma = 3/2$ also for CLT 5s and 7s beam elements, irrespective of the considered lay-ups, as the highest possible value according to Eq. (28). In this case, design relevant torsional shear stress for CLT 3s, 5s and 7s with beam orientation $L$ may be calculated as follows

$$\tau_{\text{tor},j} = \frac{9}{2}\frac{V}{b_x^2}\frac{1}{n_{\text{CA},k}}\frac{t_{x,k}}{t_x}\left(\frac{b_x}{h} - \frac{b_x^3}{h^3}\right)k_b \tag{29}$$

One additional proposal for calculation of the design-relevant torsional shear stress at in-plane beam loading conditions is suggested here, to allow for a unified formulation of design equations for both pure in-plane shear loading and in-plane beam loading conditions. Considering the expression for the torsional shear stress according to Eq. (19) and using the approximation $\alpha_{\text{max,approx},3}$ according to Eq. (25) gives the following expression for the design-relevant torsional shear stress

$$\tau_{\text{tor},j} = \frac{3V}{b_x^2}\left(\frac{3}{2}\frac{b_x}{h}k_{1,j} - \frac{1}{n_{\text{CA},k}}\frac{t_{x,k}}{t_x}\frac{b_x^3}{h^3}\right)k_b \tag{30}$$

where $j$, $k$ and $n_{\text{CA},k}$ should be used as in Eq. (12) and with $k_{1,j}$ and $k_b$ according to Eqs. (8) and (9), respectively.

CLT beams with a large number of laminations in the beam heigt direction ($m = h/b$ greater than 8) gives $b_x/h \gg {b_x}^3/h^3$. By expressing the mean shear flow over the beam height as $v_{xy} = V/h$, Eq. (30) can then be rewritten as

$$\tau_{\text{tor},j} = \frac{3}{2}\frac{3v_{xy}}{b_x}k_{1,j}k_b \tag{31}$$

which corresponds to the expression in Eq. (7) multiplied by 3/2, indicating a uniform design approach, but reflecting the difference between the even shear distribution in the pure shear case and the parabolic distribution for the beam loading case.

Comparisons between FE-results reviewed in Section 3.2 and model predictions for design-relevant stresses, $\tau_{zx,\text{max}}$ and $\tau_{\text{tor,max}}$, are presented in Fig. 8 assuming equal laminations widths $b_x = b_y = 150$ mm and total number of laminations in the beam heigt direction $m = h/b_x = 4$. Design-relevant stresses were determined by equations presented above, as indicated in Fig. 8, considering each crossing area in the beam width direction ($j = 1$ and 2 for CLT 5s and $j = 1$, 2 and 3 for CLT 7s) and adopting only the maximum value. Results indicate fair agreement between FE-results and model B predictions, as concluded above in Section 3.2, but also reasonable agreement with several design proposals based on model B. For some proposals, the gain from more accurate stress predictions compared to FE-analysis comes at the price of more complicated design equations. However, all of them are predicting higher values of design relevant stresses compared to FE-results, indicating their conservative aspect.

## 4. Unified design proposal for in-plane shear and beam loading conditions

The analytical models for stress analysis of pure in-plane shear loading and in-plane beam loading conditions, presented above, can be used to formulate a unified design approach for the two loading cases. Using these rationally based models and introducing the above-mentioned simplifications, yields the following proposal for a unified design approach and calculation of design-relevant stresses for shear failure mode III in CLT. The design proposal is based on Eq. (7) for the torsional shear stress at pure in-plane shear loading and on Eqs. (22) and (30) for the shear stress components at in-plane beam loading conditions. The element lay-up is in this design proposal considered by the factors $k_{1,j}$ and $k_{2,j}$.

CLT at pure in-plane shear loading:

The torsional stress component for crossing area $j$ can be determined according to

$$\tau_{\text{tor},j} = \frac{3v_{xy}}{b_x}k_{1,j}k_b \tag{32}$$

where the factor $k_{1,j}$ is given by

$$k_{1,j} = \begin{cases} j = 1\,;\ \left\{\frac{1}{2}\right\} & \text{for CLT 3s} \\ j = 1,\ 2\,;\ \left\{\frac{t_{x,1}}{t_x},\ \frac{1}{2}\frac{t_{x,2}}{t_x}\right\} & \text{for CLT 5s} \\ j = 1,\ 2,\ 3\,;\ \left\{\frac{t_{x,1}}{t_x},\ \frac{t_{y,1}}{t_y} - \frac{t_{x,1}}{t_x},\ \frac{1}{2} - \frac{t_{y,1}}{t_y}\right\} & \text{for CLT 7s} \end{cases} \tag{33}$$

and where the factor $k_b$ is defined according

$$k_b = \frac{2b_{\text{max}}b_x}{b_x^2 + b_y^2} \tag{34}$$

with $b_{\text{max}} = \max(b_x, b_y)$.

CLT at in-plane beam loading:

The stress components to be considered in design can be determined according to

$$\tau_{\text{tor},j} = \frac{3V}{b_x^2}\left(\frac{3}{2}\frac{b_x}{h}k_{1,j} - \frac{b_x^3}{h^3}k_{2,j}\right)k_b \tag{35}$$

$$\tau_{zx,j} = \frac{6V}{h^3}b_x k_{2,j} \tag{36}$$

with $k_{1,j}$ according to Eq. (33), $k_b$ according to Eq. (34) and where the factor $k_{2,j}$ is given by

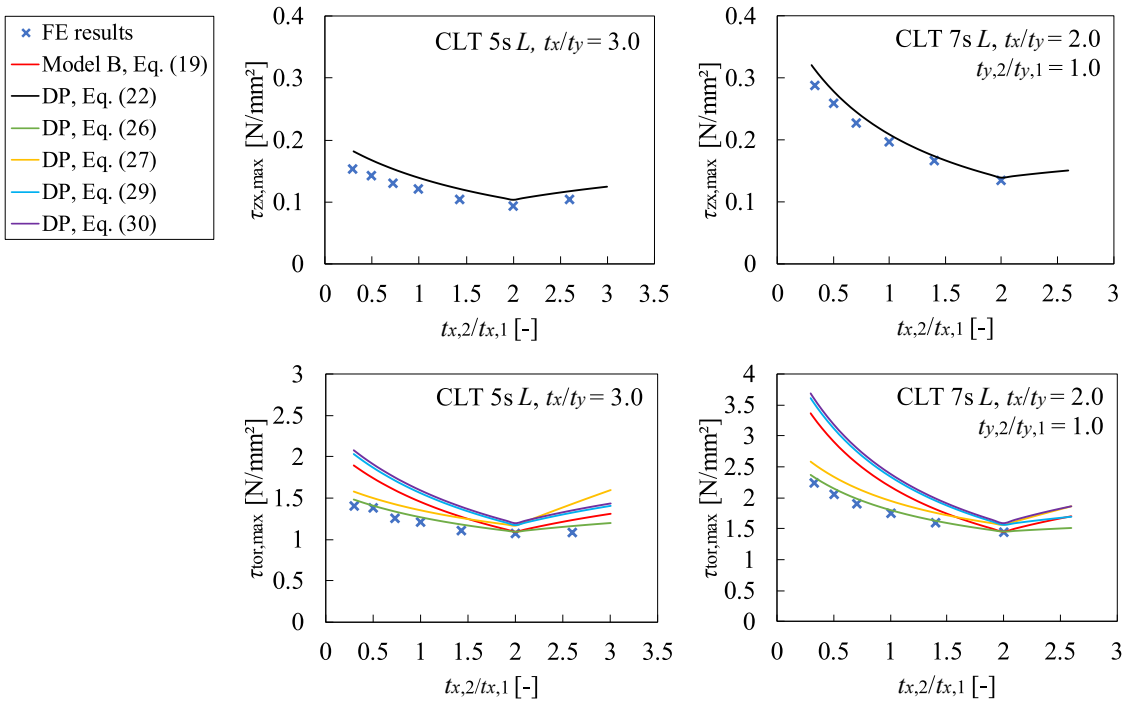


**Fig. 8.** Comparison between FE results and model predictions for design relevant stresses for varing lay-ups $0.31 \leq t_{x,2}/t_{x,1} \leq 2.6$ of CLT 5s and $0.33 \leq t_{x,2}/t_{x,1} \leq 2.0$ of CLT 7s.

$$k_{2,j} = \begin{cases} j = 1\,;\ \left\{\frac{1}{2}\right\} & \text{for CLT 3s} \\ j = 1,\ 2\,;\ \left\{\frac{t_{x,1}}{t_x},\ \frac{1}{2}\frac{t_{x,2}}{t_x}\right\} & \text{for CLT 5s} \\ j = 1,\ 2,\ 3\,;\ \left\{\frac{t_{x,1}}{t_x},\ \frac{1}{2}\frac{t_{x,2}}{t_x},\ \frac{1}{2}\frac{t_{x,2}}{t_x}\right\} & \text{for CLT 7s} \end{cases} \tag{37}$$

Design-relevant stresses for pure in-plane shear and beam loading conditions, $\tau_{\text{tor},j}$ and $\tau_{zx,j}$, have to be calculated in the general case for each crossing area $j$ in the beam width direction and the maximum values should be used in design verification, i.e. in the respective failure criteria. This is however only necessary for CLT 5s and 7s elements while in the case of CLT 3s only one crossing area ($j = 1$) needs to be verified. However, for practically relevant lay-ups of CLT 5s elements with $t_{x,2}/t_{x,1} \leq 2.0$, stress verification need only to be done for the outermost (critical) crossing area ($j = 1$) of the external longitudinal laminations ($k = 1$). In the case of CLT 7s it is not so straightforward to define the critical crossing area due to dependence on both longitudinal and transversal relative thicknesses, i.e. $t_{x,2}/t_{x,1}$ and $t_{y,2}/t_{y,1}$. However, for practically relevant lay-ups of CLT 7s elements with $t_{x,2}/t_{x,1} \leq 2.0$ and equal transversal layer thickness $t_{y,2}/t_{y,1} = 1.0$, stress verification needs only to be done for the outermost crossing area ($j = 1$) of the external longitudinal laminations ($k = 1$). For other ratios of $t_{y,2}/t_{y,1}$, crossing areas for internal longitudinal laminations ($j = 2$ and 3) should be also considered.

## 5. Conclusions and outlook

Unified and consistent design proposals for in-plane shear and beam loading conditions are presented based on the same rational mechanical background, but taking into account the difference between the even shear distribution in the pure shear case and the parabolic distribution for the beam loading case. Presented design proposals show overall good agreement with FE-results where both are predicting higher values of design-relevant stresses, indicating their conservative aspect.

However, some limitations and assumptions are introduced. The presented unified design proposals are based on a macroscale material level considering equal and homogeneous material for all laminations. Possible effects on the lamination strength and stiffness by splitting of laminations, e.g. influence of knots and knot placement, are hence not taken into account. Further assumptions are related to the adopted crossing area shear stress distributions, see Fig. 2 and Fig. 4, and the adopted failure criterion found in literature, i.e. $\tau_{\text{tor,max}}/f_{v,\text{tor}} \leq 1.0$ for pure in-plane shear and $\tau_{\text{tor,max}}/f_{v,\text{tor}} + \tau_{zx}/f_r \leq 1.0$ for in-plane beam loading conditions. Such failure criteria are based on a simplified linear elastic approach where verification is done on only one single critical crossing area.

Another aspect is related to the origin of the in-plane shear stress components acting in the crossing areas, which from a theoretical point of view, is irrelevant. Namely, the shear capacity is expressed in terms of the sum of the shear stress along the direction of the beam (rolling shear) and a torsional shear stress, and for these two contributions, different strength values are applied. The torsional shear strength $f_{v,\text{tor}}$ should in this sense be understood as a *fictitious* strength parameter which is strongly related to the structural properties, rather than a material property as in a conventional strength-of-materials approach. In a continuum-based approach, the stress situation would be described by two perpendicular shear stress components acting in the crossing area, $\tau_{zx}$ and $\tau_{zy}$, without taking into account the loading situation provoking these stresses. Other approaches for verification of load-bearing capacity could be favourable, e.g. using failure criteria based on only the rolling shear strength as discussed in [18,29] or using approaches based on fracture mechanics.

The design proposals are based on the assumption of equal longitudinal lamination width $b_x$ in the element height direction. This is mostly relevant for beam elements, since dimensions and placement of individual laminations with respect to the element edges are generally not known in the actual design situation as beams typically are cut from larger CLT panels with no consideration of the location of the element edges in relation to the edges of the individual laminations. However, as shown by Jeleč et al. [17,27,28], a reduced lamination width close to the edges for CLT 3s, 5s and 7s beam elements indicate a relatively small influence on predicted shear capacity with respect to failure in the

crossing areas (mode III). Compared to the reference cases with equal widths for all longitudinal laminations, the differences in predicted stress ratio $\tau_{tor,max}/f_{v,tor} + \tau_{zx}/f_r$, see Eq. (10), for reduced widths of the upper- and lowermost laminations are not more than 2 % for CLT 3s, 5 % for CLT 5s and 6 % for CLT 7s. Lamination widths $b_x$ and $b_y$ are in ETAs commonly stated as an interval, typical ranging from 80 mm to 250 mm. In cases where the lamination width is not known, a conservative approximation as $b_x = b_y = 80$ mm may be assumed, following the recommendation in the draft version of the new Eurocode 5 (CEN/TC 250/SC5, 2021) [22].

Further investigations of CLT beam elements with outer laminations parallel to the vertical direction (beam orientation *T*) should preferably also be conducted, since some differences in weighting factors in beam width direction could be expected. As mentioned in Section 1, such layer orientation would be relevant for lintels in continuous CLT elements with cut-outs for windows and doors. In order to determine a complete unified design proposal for CLT at in-plane shear and beam loading conditions, irrespective of the orientation of outer laminations for beam elements, further experimental and numerical investigations are hence needed.

## CRediT authorship contribution statement

**Henrik Danielsson:** Conceptualization, Methodology, Formal analysis, Validation, Funding acquisition, Writing – original draft, Writing – review & editing. **Mario Jeleč:** Conceptualization, Methodology, Formal analysis, Validation, Writing – original draft, Writing – review & editing.

## Declaration of Competing Interest

The authors declare that they have no known competing financial interests or personal relationships that could have appeared to influence the work reported in this paper.

## Data availability

Data will be made available on request.

## Acknowledgments

The financial support from FORMAS for the project *Strength and fracture analysis of cross laminated timber* (grant 2019-01354) and the financial support for the project *InnoCrossLam* is gratefully acknowledged. The project *InnoCrossLam* is supported under the umbrella of ERA-NET Cofund ForestValue and has recieved finacial support from the Swedish Governmental Agency for Innovation Systems, the Swedish research council FORMAS and the Swedish Energy Agency. ForestValue has received funding from the European Union's Horizon 2020 research and innovation programme under grant agreement N° 773324.

## References

[1] M. Jeleč, D. Varevac, V. Rajčić, Cross-laminated timber (CLT): a state of the art report, Građevinar 70 (2) (2018) 75–95.
[2] R. Brandner, G. Flatscher, A. Ringhofer, G. Schickhofer, A. Thiel, Cross laminated timber (CLT): overview and development, Eur. J. Wood Wood Prod. 74 (3) (2016) 331–351.
[3] H. Kreuzinger, M. Sieder, Einfaches Prüfverfahren zur Bewertung der Schubfestigkeit von Kreuzlagenholz/Brettsperrholz, Bautechnik 90 (5) (2013) 314–316.
[4] EN 16351 Timber Structures – Cross Laminated Timber – Requirements. European Committee for Standardization (CEN), 2021.
[5] R. Brandner, P. Dietsch, J. Dröscher, M. Schulte-Wrede, H. Kreuzinger, M. Sieder, Cross laminated timber (CLT) diaphragms under shear: Test configuration, properties and design, Constr. Build. Mater. 147 (2017) 312–327.
[6] T. Bogensperger, T. Moosbrugger, G. Silly, Verification of CLT-plates under loads in plane, in: Proc. WCTE, Riva del Garda, Italy, 2010.
[7] M. Wallner-Novak, J. Koppelhuber, K. Pock, Brettsperrholz Bemessung – Grundlagen für Statik und Konstruktion nach Eurocode, ProHolz Austria, Druck Eberl Print, Immenstadt, Austria, 2013.
[8] ÖNORM B 1995-1-1 /A:2018-11: Eurocode 5: Design of timber structures – Part 1-1: General – Common rules and rules for buildings – National specifications for the implementation of ÖNORM EN 1995-1-1, national comments and national supplements (Amendment), Austrian Standards International, 2018.
[9] H. Danielsson, E. Serrano, Cross laminated timber at in-plane shear loading – Comparison of model predictions, in: Proc. INTER, INTER/52-12-2, Tacoma WA, USA, 2019.
[10] H. Danielsson, M. Jeleč, E. Serrano, Prediction of torsional stress at in-plane shear loading of cross laminated timber, in: Proc. INTER, INTER/53-12-3, Online Meeting, 2020.
[11] H.J. Blass, M. Flaig, Stabförmige Bauteile aus Brettsperrholz, KIT, Karlsruhe, Germany, 2012.
[12] M. Flaig, H.J. Blass, Shear strength and shear stiffness of CLT-beams loaded in plane, in: Proc. CIB-W18, CIB-W18/46-12-3, Vancouver, Canada, 2013.
[13] H. Danielsson, E. Serrano, Cross laminated timber at in-plane beam loading – Prediction of shear stresses in crossing areas, Eng. Struct. 171 (2018) 921–927.
[14] M. Jeleč, H. Danielsson, E. Serrano, V. Rajčić, Cross laminated timber at in-plane beam loading – New analytical model predictions and relation to EC5, in: Proc. INTER, INTER/51-12-5, Tallinn, Estonia, 2018.
[15] H. Danielsson, M. Jeleč, E. Serrano, V. Rajčić, Cross laminated timber at in-plane beam loading – Comparison of model predictions and FE-analyses, Eng. Struct. 179 (2019) 246–254.
[16] H. Danielsson, E. Serrano, M. Jeleč, V. Rajčić, In-plane loaded CLT beams – Tests and analysis of element lay-up, in: Proc. INTER, INTER/50-12-2, Kyoto, Japan, 2017.
[17] M. Jeleč, H. Danielsson, V. Rajčić, E. Serrano, Experimental and numerical investigations of cross laminated timber at in-plane beam loading conditions, Constr. Build. Mater. 206 (2019) 329–346.
[18] H. Danielsson, E. Serrano, Cross laminated timber at in-plane shear loading – Strength and fracture analysis of shear mode III, in: Proc. WCTE, Santiago, Chile, 2021.
[19] H.J. Blass, R. Görlacher, Zum Trag- und Verformungsverhalten von LIGNOTREND Elementen bei Beanspruchung in Plattenebene, Lehrstuhl für Ingenieurholzbau und Baukonstruktionen, Universität Karlsruhe (TH), 2002.
[20] R. Jöbstl, T. Bogensperger, G. Schickhofer, G. Jeitler, Mechanical behaviour of two orthogonally glued boards, in: Proc. WCTE, Lahti, Finland, 2004.
[21] M. Flaig, N. Meyer, A new test configuration to determine the slip modulus of connections between crosswise bonded boards, in: Experimental Research with Timber, Proceedings of Cost Action FP 1004, Prague, Czech Republic, 2014.
[22] CEN/TC 250/SC5: Working draft of Eurocode 5: Design of timber structures – Common rules and rules for buildings Part 1-1: General, Version: 2021-10-27, N1488, 2021.
[23] M. Flaig, Biegeträger aus Brettsperrholz bei Beanspruch in Plattebene, PhD thesis, KIT, Karlsruhe, Germany, 2013.
[24] M. Flaig, Design of CLT beams with rectangular holes or notches, in: Proc. INTER, INTER/47-12-4, Bath, United Kingdom, 2014.
[25] M. Flaig, H.J. Blass, Bending strength of cross laminated timber loaded in plane, in: Proc. WCTE 2014, Quebec City, Canada, 2014.
[26] M. Flaig, In Plattenebene beanspruchte Biegeträger aus Brettsperrholz – Teil 1: Effektive Festigkeits und Steifigkeitskennwerte für die Schubbemessung, Bautechnik 92 (11) (2015) 741–749.
[27] M. Jeleč, Shear resistance of cross-laminated timber beam elements, PhD Thesis. Faculty of Civil Engineering, University of Zagreb, 2019.
[28] M. Jeleč, T. Dokšanović, H. Draganić, V. Rajčić, Cross laminated timber at in-plane beam loading – Advancement in prediction of shear strength and stiffness of cross laminated timber beams, Eng. Struct. 238 (2021) 112247.
[29] E. Serrano, Test methods for in-plane shear tests of cross laminated timber, in: R. Brandner, R. Tomasi, et al. (Eds.), Properties, Testing And Design of Cross LAminAted Timber: A StAte-of-the-Art Report by COST Action FP1402/WG2, Shaker Verlag, Aachen, Germany, 2018.